Available online at www.sciencedirect.com

ScienceDirect

Geochimica et Cosmochimica Acta 248 (2019) 242–251

Geochimica et Cosmochimica Acta

www.elsevier.com/locate/gca

Precise determination of equilibrium sulfur isotope effects during volatilization and deprotonation of dissolved H_2S

Min Sub Sim [a,b,*], Alex L. Sessions [b], Victoria J. Orphan [b], Jess F. Adkins [b]

[a] School of Earth and Environmental Sciences, Seoul National University, Seoul 08826, South Korea
[b] Division of Geological and Planetary Sciences, California Institute of Technology, Pasadena, CA 91125, USA

Received 16 June 2018; accepted in revised form 9 January 2019; available online 14 January 2019

Abstract

Sulfide (H_2S, HS^-, and S^{2-}) is ubiquitous in marine porewaters as a result of microbial sulfate reduction, constituting the reductive end of the biogeochemical sulfur cycle. Stable isotopes have been widely used to constrain the sulfur cycle, because the redox transformations of sulfur compounds, such as microbial sulfate reduction, often exhibit sizable kinetic isotope effects. In contrast to sulfate ion (SO_4^{2-}), the most abundant form of dissolved sulfur in seawater, H_2S is volatile and also deprotonated at near neutral pH. Equilibrium isotope partitioning between sulfide species can therefore overlap with kinetic isotope effects during reactions involving sulfide as either reactant or intermediate. Previous experimental attempts to measure equilibrium fractionation between H_2S and HS^- have reached differing results, likely due to solutions of widely varying ionic strength. In this study, we measured the sulfur isotope fractionation between total dissolved sulfide and gaseous H_2S at 20.6 $\pm$ 0.5 °C over the pH range from 2 to 8, and calculated the equilibrium isotope effects associated with deprotonation of dissolved H_2S. By using dilute solutions of Na_2S, made possible by the improved sensitivity of mass spectrometric techniques, uncertainty in the first dissociation constant of H_2S due to ionic strength could be better controlled. This in turn allowed us to close sulfur isotope mass balance for our experiments and increase the accuracy of the estimated fractionation factor. At equilibrium, aqueous H_2S was enriched in ^{34}S by 0.7‰ and 3.1‰ relative to gaseous H_2S and aqueous HS^-, respectively. The estimated fractionation between aqueous H_2S and HS^- lies between two earlier experimental reports, but agrees within the uncertainty of the measurements with a recent theoretical calculation.

Keywords: Sulfur isotopes; Equilibrium; Isotope effect; Hydrogen sulfide; Bisulfide

1. INTRODUCTION

Hydrogen sulfide (H_2S) and its deprotonated anions HS^- and S^{2-} contain sulfur in its lowest oxidation state of −2. This sulfide system, along with sulfate in the +6 oxidation state, is one of the two most abundant dissolved sulfur compounds in natural aqueous and sedimentary environments. In particular, sulfide is always present in the anoxic zone of marine sediments as a byproduct of dissimilatory sulfate reduction. It is also a reactive chemical that binds with iron and leads to the permanent burial of sulfur as pyrite (Berner, 1984), the main global sink for sulfur in the modern sulfur cycle. Depending on the availability of light or thermodynamically-favored electron acceptors such as oxygen or nitrate, sulfide can also serve as an electron donor for microbial metabolisms (Jørgensen and Nelson, 2004). Thus, sulfide is a pivotal component of the global sulfur cycle that is closely linked to those of other essential elements such as oxygen, carbon, and iron (Berner, 1989; Canfield and Raiswell, 1999).

Measurable kinetic or equilibrium isotope effects accompany most of the chemical transformations of sulfur, and

* Corresponding author at: School of Earth and Environmental Sciences, Seoul National University, Room 606, Building 25-1, 1 Gwanak-ro, Gwanak-gu, Seoul 08826, South Korea.
E-mail address: mssim@snu.ac.kr (M.S. Sim).

https://doi.org/10.1016/j.gca.2019.01.016
0016-7037/

the partitioning of stable sulfur isotopes in nature has been used as an important tool for quantifying fluxes in the sulfur cycle. In low-temperature surface environments, different redox species of sulfur are commonly out of equilibrium, where kinetic isotope effects imparted by microbial enzymatic processes are superimposed on the equilibrium fractionation. For example, dissimilatory sulfate reduction discriminates against ^{34}S in favor of the lighter ^{32}S by up to 66‰ (Sim et al., 2011), leaving seawater sulfate enriched in ^{34}S by ca. 20‰ relative to the mantle-derived sulfur (Tostevin et al., 2014). In contrast to relatively slow redox reactions such as sulfate reduction, acid–base reactions take place nearly instantaneously under Earth-surface conditions, leading to (generally smaller) equilibrium isotope effects between conjugate acids and bases. Sulfide may act as either acid or base at near neutral pH, since the first dissociation constant of H_2S is close to 10^{-7}. H_2S and HS^- are thus both present in many natural aqueous and sedimentary environments, particularly including marine systems. Given that many reactions use one particular aqueous species as reactant, not total dissolved sulfide, the equilibrium fractionation between species must therefore play a role in determining the overall fractionation. The situation is very much analogous to the more familiar inorganic carbon system, where fractionations between CO_2(aq), HCO_3^-, and CO_3^{2-} are important components of the isotope effects accompanying both the fixation of CO_2(aq) by Rubisco as well as the precipitation of carbonate minerals from CO_3^{2-}.

For the sulfide system, equilibrium sulfur isotope fractionations have been explored experimentally by comparing the isotopic compositions of gaseous and total dissolved phases under different pH conditions that manipulate the proportion of the individual species (Fry et al., 1986a; Geßler and Gehlen, 1986). Theoretical studies have also used *ab initio* or density-functional theory to predict equilibrium distributions (Otake et al., 2008; Czarnacki and Hałas, 2012; Eldridge et al., 2016). Combined, these studies provide a consensus that gaseous H_2S is depleted in ^{34}S relative to aqueous H_2S at equilibrium, although the fractionation is only about 1‰ at 20 °C. For the first dissociation of H_2S, there has been no disagreement about the enrichment of heavy sulfur isotopes in H_2S relative to HS^-. However, the reported fractionations differ significantly by up to 6‰ at room temperature, and two experimental studies [Fry et al. (1986a) and Geßler and Gehlen (1986)] yielded $^{34}S/^{32}S$ fractionations of 2.6 and 4.6‰, respectively. Since the experimental determination of fractionation is based on sulfur isotope mass balance, a potential source of discrepancy results from erroneous estimation of the speciation of H_2S and HS^- based on pH. In particular, as noticed by Eldridge et al. (2016), the effect of ionic strength on the pKa$_1$ of H_2S was not accounted for in those studies. Such uncertainties become significant when investigating reactions with relatively small kinetic isotope effects that involve sulfide as a reactant at near neutral pH. For example, ^{34}S accumulates in elemental sulfur during the phototrophic oxidation of sulfide by anoxygenic purple and green sulfur bacteria (Fry et al.,1984; Fry et al., 1986b; Zerkle et al., 2009), yet the mechanistic basis of this rare example of an inverse isotope effect has remained elusive. Consideration of the equilibrium partitioning of sulfur isotopes between H_2S(aq), which can diffuse across the cell-membrane, and HS^-, which cannot, may help explain this fractionation.

In the present study, we measured the equilibrium $^{34}S/^{32}S$ fractionations between H_2S(g) and total dissolved sulfide species as a function of pH, as has been done before, but using the more sensitive analytical technique of multi-collector inductively-coupled plasma mass spectrometry (MC-ICP-MS). With the improved sensitivity of this technique, sulfur isotope ratios can be measured in more dilute solutions and the influence of ionic strength on the pKa$_1$ value of H_2S can be minimized. This in turn allows us to close the sulfur isotope mass balance of our experiments much more precisely than has been previously possible, and so provide more accurate estimates of equilibrium isotope effects. The newly determined values are consistent with the most recent theoretical calculation by Eldridge et al. (2016), which when combined together provide a fundamental basis for investigating the fate of sulfide in a variety of biological and chemical processes.

2. METHODS

Equilibrium sulfur isotope fractionation between H_2S gas and total dissolved sulfide ($\Sigma H_2S(aq) = H_2S(aq) + HS^- + S^{2-}$) was measured in a closed system that consisted of 100 ml (equilibration reservoir) and 500 ml (gas-collecting) flasks connected by high vacuum valve adapters with O-ring joints (Fig. 1). Each flask had two additional ports with screw-threaded and crimp-locked ends, and the total reactor volume (725 ml) was determined by measuring

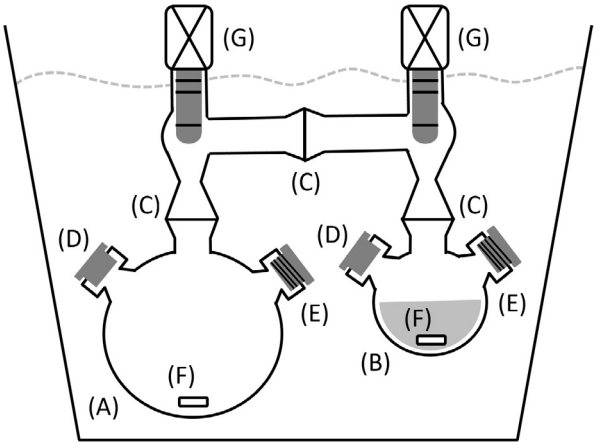

Fig. 1. A schematic diagram of the closed-system equilibrium apparatus. The temperature was maintained at 20.6 ± 0.5 °C by circulating water from a constant temperature bath around the reaction apparatus. Stirring was accomplished by a magnetic stirrer placed beneath the bath directly below the flask containing Na_2S solution. (A) 500 ml flask for collecting gaseous H_2S; (B) 100 ml flask containing 50 ml of Na_2S solution; (C) 15 mm O-ring joint with a screw locking clamp; (D) Septa port with 20 mm butyl-rubber stoppers; (E) 15 mm thread neck; (F) PTFE-coated magnetic stirring bar and (G) Teflon high vacuum stopcock.

the volume of water required to fill it. Prior to each experiment, all glassware, PTFE-coated magnetic stir bars, and butyl-rubber stoppers were placed in an anaerobic chamber (95% N_2, 5% H_2; Coy Manufacturing Co., Ann Arbor, MI, USA) for at least two days to remove all traces of O_2. The anaerobic atmosphere of the chamber was circulated through a palladium catalyst that reacts any free O_2 with H_2 to form water, which was removed by the desiccant. With stir bars in both flasks, an experimental set-up then comprised 45 ml deoxygenated water in the 100 ml flask. Water was purified using a Millipore Milli-Q system (18.2 MΩ/cm), purged with 99.99% N_2 for 30 min at room temperature, and then aged for a week in the anaerobic chamber. Purified, deoxygenated water contained no detectable sulfur species other than trace levels of sulfate (<1 μM, by ion chromatography). After compressing O-ring joints and sealing side ports, 5 ml of 100 mM sulfide stock solution was injected *via* a 5 ml syringe, and depending on the desired pH, different volumes of 1 M deoxygenated HCl was added. Deoxygenation was accomplished by flushing the sealed bottle containing 100 ml of 1 M HCl with 99.99% N_2 for 20 min. The sulfide stock solution was prepared from $Na_2S{\cdot}9H_2O$ (ACS reagent grade, Sigma-Aldrich, MO, USA), and its sulfur isotope composition was sampled by fixing 0.1 ml of the stock solution with 0.2 ml of 1 M zinc acetate to precipitate ZnS. To avoid potential contamination by oxidation products, individual crystals of $Na_2S{\cdot}9H_2O$ were rinsed briefly with ultrapure water, wiped dry with low-lint tissues, and dissolved in deoxygenated water under an N_2 atmosphere. Also, small batches of $Na_2S{\cdot}9H_2O$ (5 g) were purchased and used for the isotope equilibrium experiments to prevent oxidation during extended storage, and each had slightly different sulfur isotope ratios (Table 1). Equilibrium experiments were conducted in dilute solutions with ionic strength <0.03 M, except for one experiment performed with 0.5 M NaCl. After being assembled and filled, the experimental apparatus was transferred out of the anaerobic chamber and submerged in a water bath where the temperature was maintained at 20.6 ± 0.5 °C with a Neslab RTE-101 water circulator (Neslab, NH, USA). The sulfide system was equilibrated for one week with the solution being continuously stirred. Stirring was provided by a magnetic stirrer placed beneath the bath directly below the 100 ml flask containing Na_2S solution. Since the equilibrium between dissolved sulfide species is reached quite rapidly (Eigen and Kustin, 1960), the equilibration time was chosen based on the time scale for equilibration between gas-phase and dissolved H_2S. Fry et al. (1986a) achieved chemical and isotopic equilibrium among sulfide species within four days, and consistent results were obtained under our experimental conditions. At low pH (<3.5), the $\delta^{34}S$ value of H_2S(g) remained unchanged within the analytical uncertainty (±0.2‰) upon extension of the equilibration time from 4 to 7 to 13 days, although equilibration times as short as one day yielded inconsistent results. Leakage and oxygen intrusion was tested with parallel experiments using a redox sensitive dye, as follows. 100 ml of N_2-purged resazurin solution (1 mg/L) was added to the gas-collecting flask, which was further reduced to col-

Table 1
Fractionation of sulfur isotopes between H_2S(g) and ΣH_2S(aq) over a range of pH. The mole-weighted average of gaseous and dissolved sulfide isotope compositions is consistent with the $\delta^{34}S$ values of initial Na_2S, where data is available, confirming that the $\delta^{34}S$ mass balance is retained within the precision of measurements.

pH	T (°C)	$[Na_2S]_T$ (M)	$[NaCl]_T$ (M)	H_2S(g) relative to total sulfide (mol/mol)	$\delta^{34}S$ (‰)			$\alpha_{g\text{-}aq}$	$\varepsilon_{g\text{-}aq}$ (‰)	pKa_1*
					Na_2S	H_2S(g)	ΣH_2S(aq)	weighted average		
1.96	20.8	0.01	0	0.80 ± 0.01	18.8	18.6	19.3	18.7 ± 0.3	0.9993 ± 0.0003	−0.7 ± 0.3	6.92
2.36	20.4	0.01	0	n.d.	n.d.	18.4	19.2	n.d.#	0.9992 ± 0.0003	−0.8 ± 0.3	6.94
2.44	20.3	0.01	0	n.d.	n.d.	18.8	19.4	n.d.	0.9994 ± 0.0003	−0.6 ± 0.3	6.94
6.12	20.9	0.01	0	0.80 ± 0.01	18.4	18.5	18.8	18.6 ± 0.3	0.9997 ± 0.0003	−0.3 ± 0.3	6.94
6.98	20.6	0.01	0	0.69 ± 0.02	18.4	18.8	17.9	18.5 ± 0.4	1.0009 ± 0.0003	0.9 ± 0.3	6.95
7.21	20.1	0.01	0	n.d.	19.3	20.3	18.9	n.d.	1.0014 ± 0.0003	1.4 ± 0.3	6.95
7.47	20.6	0.01	0.5	0.51 ± 0.02	18.2	19.1	17.3	18.2 ± 0.5	1.0018 ± 0.0003	1.8 ± 0.3	6.72
7.61	21.1	0.01	0	0.51 ± 0.02	18.3	19.3	17.4	18.3 ± 0.5	1.0019 ± 0.0003	1.9 ± 0.3	6.94
7.82	20.3	0.01	0	0.43 ± 0.02	18.4	19.6	17.5	18.4 ± 0.5	1.0020 ± 0.0003	2.0 ± 0.3	6.95
7.84	20.4	0.01	0	0.46 ± 0.02	18.2	19.5	17.4	18.3 ± 0.5	1.0020 ± 0.0003	2.0 ± 0.3	6.95
8.12	20.2	0.01	0	n.d.	18.9	21.2	19.0	n.d.	1.0021 ± 0.0003	2.1 ± 0.3	6.95

#n.d., not determined.
* The acid dissociation constant under the experimental conditions was taken from Hershey et al. (1988).

orless hydroresorufin with 60 μM Ti(III)-NTA. While the assembled set-up was left in laboratory air for 20 days, the solution remained colorless, confirming the adequacy of sealing. Resazurin was not added to the incubations that were sampled for sulfur isotope analyses.

At the end of equilibration, vacuum valves were closed and the two flasks were detached from each other. 10 ml of 0.5 M $ZnCl_2$ solution, deoxygenated *via* N_2 bubbling and aging in a reducing atmosphere (95% N_2, 5% H_2), was injected to the gas-collecting flask, and the solution was stirred with a magnetic stirrer for four days to completely convert all H_2S(g) to ZnS. For analysis of ΣH_2S (aq) a 5 ml aliquot was taken from the equilibrium flask and mixed with 1 ml of 1 M zinc acetate solution, precipitating dissolved sulfide as ZnS. Solution pH was measured with a sulfide-resistant pH sensor InPro 3250 (Mettler Toledo, OH, USA). The partitioning of sulfide between gas and aqueous phases was calculated by quantifying the collected ZnS *via* a modified methylene blue assay (Cline, 1969). For sulfur isotope analysis of total, gaseous, and aqueous sulfide, ZnS were washed with deionized water (DW) three times and oxidized to sulfate in 30% H_2O_2 at 75 °C for 24 h. Sulfate as a possible minor contaminant in the sulfide stock solution, if any, should be eliminated by washing with DW, given that $ZnSO_4$ is extremely soluble in water (>50 g/100 g H_2O; Lide, 2006). Quantitative conversion of zinc sulfide to sulfate by H_2O_2 was previously described in Raven et al. (2016) and Sim et al. (2017). After oxidation and drying, samples were dissolved in 5 mM HCl, and loaded onto AG1X8 anion exchange resin. Cations were removed by rinsing the resin with 3 ml of DW four times, and sulfate was eluted with 3.6 ml of 0.5 M HNO_3 (Paris et al., 2014). Samples containing dissolved sulfate were dried on a hot plate and diluted in 5% HNO_3 to a sulfate concentration of 20 μM to match the in-house Na_2SO_4 working standard. NaOH was then added to yield equimolar Na and SO_4^{2-}.

Isotopic analyses were conducted on a Thermo Fischer Scientific Neptune Plus MC-ICP-MS, operated in medium resolution following the method described by Paris et al. (2013) and Sim et al. (2017). Samples were introduced to plasma *via* an ESI PFA-50 nebulizer and Cetac Aridus II desolvator. Sulfur isotope ratios of the sample and working standard were measured in alternating 50 cycles of 4.194 s integration time, and the instrumental blank was estimated after each sample block. The mean blank value was subtracted from the signal for each mass, and the measured $^{34}S/^{32}S$ ratios were calibrated using a linear interpolation between the two bracketing standard values. Sulfur isotope ratios are reported here using the conventional delta notation:

$$\delta^{34}S = \frac{R_{sample}}{R_{VCDT}} - 1 \quad (1)$$

where R_{sample} and R_{VCDT} are the isotope ratios ($^{34}S/^{32}S$) of a sample and the Vienna Canyon Diablo Troilite (VCDT) standard, respectively. Our working standard was calibrated against the IAEA S-1 reference material ($\delta^{34}S_{VCDT} = -0.3‰$) and has a $\delta^{34}S$ value of −1.55‰ ± 0.16 (2σ) on the VCDT scale. Analytic reproducibility of this MC-ICP-MS for $\delta^{34}S$ has been previously evaluated as $2\sigma = 0.2‰$ (Paris et al., 2013). Equilibrium fractionation factors (α) between two species A and B were calculated by:

$$\alpha_{A-B} = \frac{R_A}{R_B} = \frac{\delta^{34}S_A + 1}{\delta^{34}S_B + 1} \quad (2)$$

and the related isotopic enrichment factor (ε) is defined as:

$$\varepsilon_{A-B} = \alpha_{A-B} - 1. \quad (3)$$

In natural processes, where ε values are small, the difference in $\delta^{34}S$ values between two species A and B is a good approximation for the enrichment factor.

3. RESULTS

The sulfur isotope fractionation between H_2S(g) ($\delta^{34}S_g$) and ΣH_2S(aq) ($\delta^{34}S_{aq}$) was measured as a function of pH from 2.0 to 8.1 (Table 1). The equilibrium isotope partitioning between H_2S(g) and H_2S(aq) was estimated directly under acidic conditions (pH < 3), and the equilibrium sulfur isotope fractionation during H_2S(aq) deprotonation was calculated based on the sulfur isotope mass-balance at near-neutral pH, where both H_2S(aq) and HS^-(aq) are the dominant sulfide species. To verify the closure of isotope mass balance at different pH levels, the mole-weighted average of gaseous and dissolved sulfide isotope compositions was evaluated and compared with the $\delta^{34}S$ values of initial Na_2S. Sulfur isotope mass balance was retained within the precision of our measurements where data was available (Table 1), again consistent with no significant sulfide loss due to oxidation or leakage. Under acidic conditions, ^{34}S was enriched in solution with respect to the gas phase, while the fractionation was reversed at pH greater than the pKa_1 of H_2S. With increasing pH, relative enrichment of ^{34}S in the solution phase decreased in a sigmoidal manner (Fig. 2). In a low-pH solution, where all dissolved sulfide is fully protonated, the measured fractionation between gas- and aqueous-phase sulfide directly represents the fractionation ($\alpha_{g\text{-}aq}$) between H_2S(g) and H_2S(aq). At pH values near 2, the enrichment factor between H_2S gas and dissolved sulfide ($\varepsilon_{g\text{-}H2S}$) was measured to be $-0.7 \pm 0.2‰$ (2σ, $n = 3$), favoring the volatilization of $H_2{}^{32}S$ (Table 1). At higher pH, H_2S in solution is dissociated and forms HS^- and S^{2-}. The first pKa value for H_2S is agreed to be around 7, but the published pKa_2 values show a wide range of variation from 12 to 19. A gradual consensus seems to be emerging toward the high end of the estimates (Elis and Giggenbach, 1971; Giggenbach, 1971; Schoonen and Barnes, 1988; Licht et al., 1991; Housecroft and Constable, 2002; Migdisov et al., 2002). Such high pKa_2 values indicate that the presence of S^{2-} can be neglected in our experimental conditions, which ranged from pH 2.0 to 8.1. Then, a binary isotopic equilibrium between H_2S and HS^- in solution is given by:

$$F_{aq} = X \cdot F_{H_2S} + (1 - X) \cdot F_{HS^-} \quad (4)$$

where F_{aq}, F_{H2S}, and F_{HS-} are the fractional isotope abundance ($^{34}S/(^{32}S + {}^{34}S)$) of ΣH_2S(aq), H_2S(aq), and HS^-(aq), respectively, and X is the mole fraction of dissolved sulfide present as H_2S(aq). The approximate substitution of $\delta^{34}S$ values for F in Eq. (4) yields the more convenient form

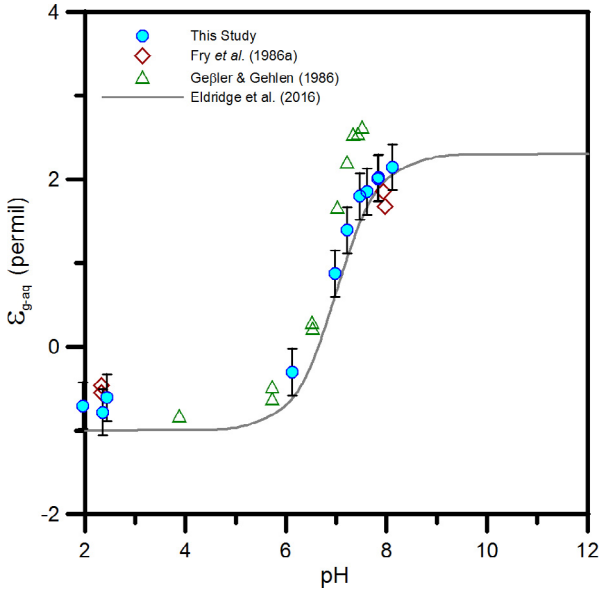

Fig. 2. Sulfur isotope fractionation between H_2S(g) and ΣH_2S(aq) at equilibrium as a function of pH. Under acidic conditions, H_2S in the gas phase is isotopically lighter than dissolved sulfide, but the fractionation is reversed as pH increases. Our estimates fall in between two prior experimental reports (Fry et al., 1986a; Geßler and Gehlen, 1986), and the solid gray line denotes the results of theoretical calculations by Eldridge et al. (2016). The vertical bars display the uncertainties propagated from the isotope measurements.

$$\delta^{34}S_{aq} = X \cdot \delta^{34}S_{H_2S} + (1-X) \cdot \delta^{34}S_{HS^-} \quad (5)$$

Because the fractional abundance (F) of ^{34}S is small (~0.044; Ding et al., 2001), and the difference between $\delta^{34}S$ values of dissolved H_2S and HS^- does not exceed 10‰, the errors introduced by this approximation are less than 0.001‰ (Hayes, 2004). Adding 1 to both sides of Eq. (5) and dividing by $(\delta^{34}S_{H_2S}+1)$ yields

$$\frac{(\delta^{34}S_{aq}+1)}{(\delta^{34}S_{H_2S}+1)} = X + (1-X) \cdot \frac{(\delta^{34}S_{HS^-}+1)}{(\delta^{34}S_{H_2S}+1)} \quad (6)$$

Multiplying the denominator and numerator in the left-hand side by $(\delta^{34}S_g+1)$ while adding and subtracting 1 in the right-hand side yields

$$\frac{(\delta^{34}S_g+1)}{(\delta^{34}S_{H_2S}+1)} \Big/ \frac{(\delta^{34}S_g+1)}{(\delta^{34}S_{aq}+1)} = 1 + (1-X) \cdot \left\{ \frac{(\delta^{34}S_{HS^-}+1)}{(\delta^{34}S_{H_2S}+1)} - 1 \right\} \quad (7)$$

Recognizing that $\alpha_{A\text{-}B} = (\delta_A+1)/(\delta_B+1)$ then yields

$$\frac{\alpha_{g-H_2S}}{\alpha_{g-aq}} = 1 + (1-X) \cdot \varepsilon_{HS^- - H_2S} \quad (8)$$

Since X is a function of pH and pKa_1, Eq. (8) can be rewritten as:

$$\frac{\alpha_{g-H_2S}}{\alpha_{g-aq}} = 1 + \left(1 - \frac{1}{1+10^{pH-pKa_1}}\right) \cdot \varepsilon_{HS^- - H_2S} \quad (9)$$

Using the fractionation factor between gas-phase and dissolved H_2S ($\alpha_{g\text{-}H2S}$) determined at low pH, the measured $\alpha_{g\text{-}aq}$ and pH values should define a straight line in $\alpha_{g\text{-}H2S}/\alpha_{g\text{-}aq}$ vs. $(1-X)$ space, so long as the assumptions in deriving this equation are upheld. For example, if the analyte incorporates the potential products of sulfide oxidation (e.g. polysulfide), the sulfur isotope data will fail to regress in a linear manner. Finally, the slope of a linear regression through the data yields the enrichment factor for the deprotonation of H_2S (Fig. 3). Assuming a pKa_1 value of 7 (Fig. 3A), the enrichment factor ($\varepsilon_{HS\text{-}H2S}$) was estimated to be −3.1‰ with a 95% CI of −2.9 to −3.4‰. Although close to 7, the pKa_1 for the dissociation of H_2S varies with temperature and ionic strength (Morse et al., 1987; Hershey et al., 1988). Under our experimental conditions, the calculated enrichment factor remains approximately constant at −3.1‰ (95% CI, −2.8 to −3.3‰) even when such variability of pKa_1 was taken into account (Fig. 3B). For each calculation, uncertainty in the value of $\varepsilon_{HS\text{-}H2S}$ was estimated *via* Monte Carlo simulation (n = 5000), which considers all known errors in pH (±0.02), temperature (±0.25 °C), and isotope measurements.

4. DISCUSSION

4.1. Experimental determination of equilibrium sulfur isotope fractionation

Considerable experimental and theoretical efforts have previously been made to determine the equilibrium isotope effect between H_2S in the gas phase and solution (Fry et al., 1986a; Geßler and Gehlen, 1986; Otake et al., 2008; Czarnacki and Hałas, 2012; Eldridge et al., 2016). The enrichment factor ($\varepsilon_{g\text{-}H2S}$) was measured to be −0.5‰ at 22 °C (Fry et al., 1986a) and −0.8‰ at 25 °C (Geßler and Gehlen, 1986), while the calculated values were slightly larger and close to −1.0‰ at 25 °C (Czarnacki and Halas, 2012; Eldridge et al., 2016). Our estimation of −0.7‰ (Table 1) confirms a consensus that ^{34}S is accumulated slightly in dissolved H_2S relative to H_2S gas at equilibrium.

Unlike the equilibrium fractionation between gaseous and dissolved H_2S, that between dissolved H_2S and HS^- cannot be directly measured because of their rapid interconversion. Sulfur isotope compositions of these two species therefore have to be calculated based on those of H_2S(g) and ΣH_2S(aq), and the acid-base equilibrium relationship between the species. The former determines the isotopic composition of dissolved H_2S, and the latter accounts for the relative abundance of H_2S and HS^- in media. Thus, the accuracy of the derived fractionation factor depends on the accuracy not only of the isotope ratios but also of the first dissociation constant (pKa_1) of hydrogen sulfide. Prior to this study, Fry et al. (1986a) and Geßler and Gehlen (1986) have attempted to determine the equilibrium fractionation associated with H_2S(aq) deprotonation, but these two experimental results disagreed by 2‰. When the isotopic fractionations between H_2S(g) and ΣH_2S(aq) are plotted as a function of pH, our estimates are intermediate between Fry et al. (1986a) and Geßler and Gehlen (1986), agreeing more with the former estimate at high

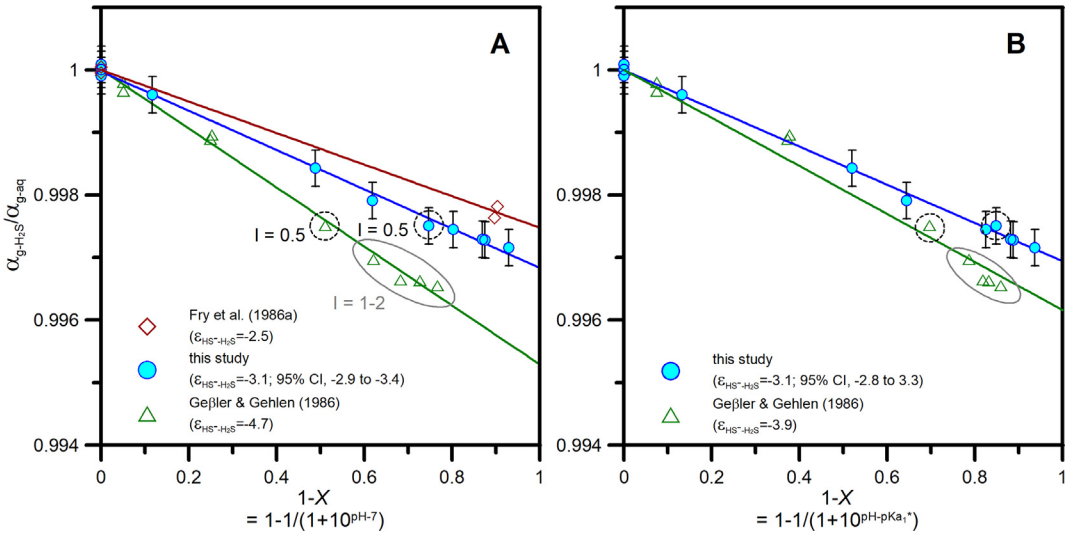

Fig. 3. Equilibrium sulfur isotope fractionation during the deprotonation of aqueous H_2S ($\varepsilon_{H2S\text{-}HS}$), obtained from the slope of $(1-X)$ versus $\alpha_{g\text{-}H2S}/\alpha_{g\text{-}aq}$ (Eqs. (8) and (9)). Data points from high ionic strength solutions are denoted by either black broken ($I = 0.5$ M) or gray solid circle ($I = 1$–2 M). (A) The first dissociation constant of H_2S is assumed to be constant at 7. (B) The effect of ionic strength on the pKa_1 of H_2S is calculated for all measured data, following the scheme proposed in Hershey et al. (1988). For the data collected in this study, the vertical bars display uncertainties propagated from the isotope measurements, while the uncertainties of $(1-X)$ are smaller than the size of symbols. The 95% CI of the regression slope is estimated *via* Monte Carlo simulation ($n = 5000$). Uncertainty analysis was not performed for literature data, because not enough information was available for the uncertainty of each variable involved.

pH and more the latter at low pH (Fig. 2). As described in the results section, the equilibrium fractionation factor between H_2S(aq) and HS^-(aq) can be obtained from the slope of $(1-X)$ versus $\alpha_{g\text{-}aq}/\alpha_{g\text{-}H2S}$. Assuming a p$Ka_1$ value of 7.0, linear regression analysis yielded the enrichment factors ($\varepsilon_{HS\text{-}H2S}$) of −2.5, −4.7, and −3.1‰ for Fry et al. (1986a), Geßler and Gehlen (1986), and this study, respectively (Fig. 3A). The observed discrepancy is too large to be ascribed to either temperature variation up to 5 °C or analytic uncertainties, which in turn suggests that the inaccuracy of the pKa_1 value might be responsible for variation across the experiments. Indeed, the first dissociation constant of H_2S changes due to both temperature and ionic strength (Hershey et al. 1988). Recently, Eldridge et al. (2016) also pointed out that Fry et al. (1986a) and Geßler and Gehlen (1986) both presumed the pKa_1 of H_2S to be very close to 7 in their experiments. But because this pKa_1 value corresponds to an ionic strength lower than 0.01 M at the given temperature (Hershey et al., 1988), any increase in ionic strength could have influenced their estimates. Although the pKa_1 values under the experimental conditions are essential for the isotope calculation, Fry et al. (1986a) did not provide enough experimental details to assess the ionic strength of their media. Moreover, they measured isotopic offsets between gaseous and dissolved sulfide at only two pH values. We therefore focus more on the comparison between our estimates and those in Geßler and Gehlen (1986) in the following discussion.

Our experimental conditions differ from those of Geßler and Gehlen (1986) in two primary aspects. First, we incubated the reaction apparatus at a 5 °C lower temperature. The second, more significant difference, is rooted in the preparation of sulfide solution and the following pH titration process. Geßler and Gehlen (1986) filled the headspace of a reactor with pure H_2S gas. Because the dissolution of hydrogen sulfide decreased the pH of media, an appropriate amount of NaOH was added depending on the desired pH. As a result, the Na^+ concentration was as high as 2 M for their high pH measurements, and the ionic strength of media varied widely from 0.01 to 2 M (Geßler and Gehlen, 1986; Eldridge et al., 2016). In our study, a more dilute sulfide solution (10 mM) was prepared from Na_2S, and as the solution was initially basic, pH was adjusted using hydrochloric acid. The resulting ionic strength remained relatively constant, ranging from 0.02 to 0.03, except for one NaCl-amended experiment. When accounting for the effect of temperature and ionic strength on the dissociation of H_2S (Hershey et al., 1988), the slope given by Geßler and Gehlen (1986) changes considerably (Fig. 3B). In the region of low pH (left side in Fig. 3B), their data apparently plot on the same line as ours, but deviate downward from it as pH, and thus ionic strength, increase. The enrichment factor could be estimated at −3.9‰ using linear regression analysis, which reduces the gap between Geßler and Gehlen (1986) and our estimates. However, such failure to obtain a straight line implies that the predicted pKa_1 values for high ionic strength media might not be accurate enough to close the isotope mass balance, and the ratios of HS^- to H_2S in media are likely underestimated. Then, the magnitude of fractionation would be overestimated. Alternatively, the failure to achieve mass balance (Eq. (9)) may suggest that non-sulfide sulfur potentially contributed to the isotopic measurement. For example, polysulfide tends to be enriched in ^{34}S relative to

sulfide (Amrani et al., 2006) and predominate as pH and ΣH_2S(aq) increase (Rickard and Luther, 2006). A detailed assessment of the experimental conditions in Geßler and Gehlen (1986) is not trivial and beyond the focus of this paper, but the deviation of experimental data from a linear trend at high pH does suggest the possibility of experimental artifacts.

In contrast, incorporation of the effect of ionic strength does not impact our estimates significantly, maintaining a straight line in the $(1-X)$ versus $\alpha_{g\text{-}aq}/\alpha_{g\text{-}H2S}$ space (Fig. 3B). Except for one NaCl-amended experiment ($I = 0.5$ M), weak ionic strength sulfide solutions ($I < 0.03$ M) were used for the experiments; therefore, the linearity suggests that in the low ionic strength range, the empirical equation for the first dissociation quotient of H_2S (Hershey et al., 1988) is precise enough to allow the determination of equilibrium fractionation between dissolved H_2S and HS^-. Also evident is that no sulfur contamination contributed considerably to the estimated equilibrium fractionation. According to linear regression analysis (Fig. 3), the sulfur isotope fractionation associated with the deprotonation of H_2S remains −3.1‰, whether the effect of ionic strength is accounted for or not. This is because the correction to pK_1 for ionic strength is very small at the low ionic strengths used in our experiments. Moreover, our estimate of -3.1 ± 0.2‰ is within uncertainty of the theoretical estimation (−3.3‰ at 20.6 °C) by Eldridge et al. (2016) that utilized sulfur molecules coordinated with 30 water molecules to approximate the effects of solvation on molecular vibration. Thus, both linearity in the $\alpha_{g\text{-}aq}/\alpha_{g\text{-}H2S}$ vs. $(1-X)$ space and consistency with the theoretical prediction support the accuracy of our estimate.

Experimental calibrations (Fry et al., 1986a; Geßler and Gehlen, 1986), including our own, have thus far focused on the determination of the sulfur isotope fractionation during deprotonation of aqueous H_2S at a single temperature. However, the close agreement between theoretical (Eldridge et al., 2016) and experimental results achieved in this study suggests that our estimate can be extrapolated over a range of temperatures (Clayton and Kieffer, 1991; Schauble, 2004), using a scaled theoretical curve based on the frequencies and their isotopic shifts calculated by Eldridge et al. (2016). We derive a scaling factor of 0.923 from the ratio of the experimental to the theoretical enrichment factors at 20.6 °C. Applying this scaling to the calculations of Eldridge et al (2016) at different temperatures, a polynomial fit to $\varepsilon_{HS\text{-}H2S}$ values in the low temperature regime (0–100 °C) is given by:

$$\varepsilon_{HS-H_2S} = -0.01108 \times \left(\frac{10^3}{T}\right)^4 + 0.13934 \times \left(\frac{10^3}{T}\right)^3 - 0.46514 \times \left(\frac{10^3}{T}\right)^2 - 0.49120 \times \left(\frac{10^3}{T}\right) \quad (10)$$

where T is temperature in Kelvin. This equation represents the equilibrium sulfur isotope fractionation during the H_2S deprotonation in most aquatic environments at Earth-surface conditions. The expected temperature dependence only changes by 0.6‰ from 0 to 100 °C.

4.2. Comparison to kinetic sulfur isotope fractionation during H_2S outgassing

Unlike sulfate, which exists as a deprotonated ion in solutions at ambient pH and temperature, the fully-protonated sulfide, H_2S(aq) acts a week acid with near-neutral pKa_1 value. In its protonated form it is volatile and can escape as a gas into the atmosphere in natural or artificial sulfidic systems such as tidelands (Bates et al., 1992), paddy fields (Zhang et al., 2004) and sewage (Yongsiri et al., 2005). Since H_2S(aq) and HS^-(aq) are isotopically distinct by 3.1‰ at equilibrium (Fig. 3), the relative ratio of these two, controlled by pH, may have a significant impact on the sulfur isotope composition of sulfide emissions, although the kinetics of the outgassing process must also be accounted for. Baune and Böttcher (2010) estimated the sulfur isotope fractionation during sulfide degassing by bubbling diluted sodium sulfide solutions with N_2 gas at pH conditions between 2.6 and 10.8, showing that the emitted H_2S(g) becomes enriched in ^{34}S as pH increases past the pKa_1 of H_2S(aq) (Fig. 4). The results of these degassing experiments are thus largely consistent with those of our equilibrium prediction. In detail, however, degassing of H_2S in acidic and near-neutral pH conditions tended to favor ^{32}S compared to our results, while the gas phase was more enriched in ^{34}S than predicted by equilibrium at basic pH. When averaged, the sulfur isotope fractionation during H_2S degassing ($\varepsilon_{g\text{-}aq}$) at low pH was −0.9‰ (Baune and Böttcher, 2010), but a rather wide scatter of individual measurements from −0.1 to −1.6‰ reflects the complex nature of their experiments (Fig. 4). There are a number of possible physical effects and experimental artifacts that could

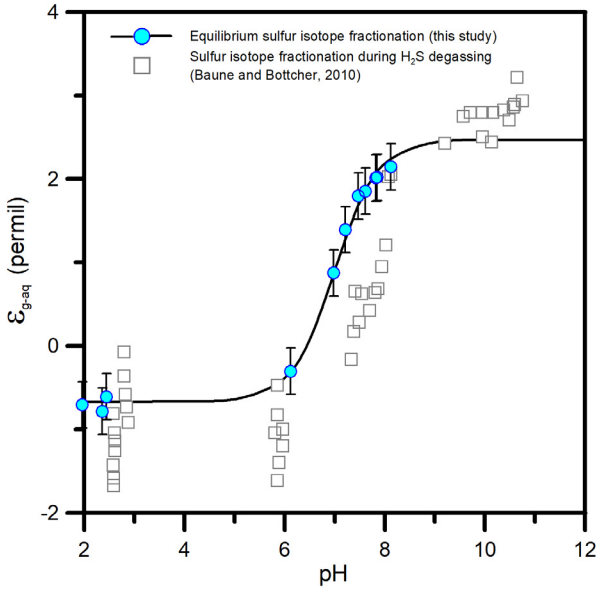

Fig. 4. Sulfur isotope fractionation between H_2S(g) and ΣH_2S(aq) during equilibrium isotope exchange (circles; this study) and outgassing by N_2 bubbling (square; Baune and Böttcher, 2010). Solid line represents the equilibrium isotope fractionation as a function of pH.

contribute to such differences, including establishment of equilibrium at a molecular-scale boundary layer, kinetic diffusion into bubbles, re-dissolution of gases from the headspace, and oxidation by traces of O_2 in the sweep gas. Given that the departure from equilibrium changes in sign from low to high pH, there is likely more than one mechanism in play.

4.3. Sulfur isotope effects during reactions involving sulfide as a reactant

Sulfide is a key participant in the biogeochemical cycle of sulfur and is produced predominantly by anaerobic microorganisms that reduce sulfate to sulfide in Earth's surface environments. Since more than 90% of microbially-produced sulfide is eventually reoxidized instead of being buried (Thamdrup et al., 1994), sulfide oxidation is one of the major pathways of the sulfur cycle. Isotopic fractionation accompanying the oxidation of reduced sulfur is typically much weaker than those accompanying sulfate reduction. Interestingly, a distinct preference for heavy sulfur isotopes (an inverse isotope effect) has been reported for the phototrophic oxidation of sulfide to elemental sulfur. Such anomalies are on the order of a few permil with a maximum fractionation of 5‰ occurring for the oxidation of sulfide by the green sulfur bacterium, *Chlorobium thiosulfatophilum* (Chambers and Trudinger, 1979; Fry et al., 1984; Fry et al., 1986b; Zerkle et al., 2009; Brabec et al., 2012). The equilibrium isotope fractionation enriching H_2S in ^{34}S relative to HS^- has been proposed as a mechanism behind the inverse sulfur isotope fractionation during phototrophic sulfide oxidation (Fry et al., 1984; Zerkle et al., 2009). In a solution of near neutral pH, where H_2S(aq) and HS^- coexist, H_2S(aq) is indeed enriched in ^{34}S relative to the total dissolved sulfide. This equilibrium distribution of isotopes could plausibly result in an inverse isotope effect if microbes preferentially utilized H_2S(aq), which freely penetrates the biological lipid bilayer (Mathai et al., 2009), whereas HS^- transport requires tightly-regulated membrane channels (Czyzewski and Wang, 2012). However, inverse fractionations that exceed the newly-determined equilibrium value of 3.1‰ have been observed. For example, neutrophilic *Chlorobaculum tepidum* and *Chlorobium thiosulfatophilum* are known to enrich in ^{34}S by 3.6‰ (Brabec et al., 2012) and 5‰ (Chambers and Trudinger, 1979), respectively, during phototrophic sulfide oxidation to elemental sulfur. The magnitudes of these inverse effects cannot be quantitatively explained solely by equilibrium effects, and require additional metabolic fractionations. It appears then that phototrophic sulfide oxidation is likely one of the rare examples of an inverse enzymatic kinetic isotope effect. A similar phenomenon has also been described for dissimilatory microbial oxidation of nitrite to nitrate (Casciotti, 2009; Buchwald and Casciotti, 2010; Brunner et al., 2013).

A more precise understanding of the equilibrium fractionation between dissolved sulfide species should also prove useful in elucidating mechanistic details of a wide variety of sulfur reactions. For example, while most organisms acquire H_2S(aq) via passive diffusion, the giant hydrothermal vent tubeworm *Riftia pachyptila* appears to actively uptake HS^- for its intracellular microbial symbionts (Goffredi et al., 1997). This distinction currently requires difficult biochemistry to establish, but might also be proven through careful sulfur isotope measurements. In the abiotic realm, HS^- is thought to be a more effective nucleophile than H_2S(aq) and hence more important reactant in the (abiotic) process of organic matter sulfurization (e.g. Jans and Miah, 2003). Although the kinetic fractionations accompanying these reactions are not yet known well enough, the equilibrium fractionation between sulfide species must play a role in their output. In the H_2S pathway to convert FeS to pyrite, it is H_2S(aq), not HS^-, that acts as an oxidant of FeS (Rickard and Luther, 1997). Thus the equilibrium partitioning between H_2S and HS^- is also part and parcel of the pyrite sulfur isotopic record.

As a final remark, we note that increasing attention has recently been paid to sulfide as a signal molecule or physiological indicator in biomedical studies (Li et al., 2011; Paul and Snyder, 2012; Szabo et al., 2013). Here, the isotopic composition of aqueous sulfide may be particularly sensitive to pH, both because human physiological pH is close to pKa_1 and because there are no large kinetic fractionations from sulfate respiratory processes to overprint subtler equilibrium effects. In human cells, sulfide is produced predominantly from cysteine or its derivatives by the enzymes cystathionine β-synthase and cystathionine γ-lyase, and released into the extracellular spaces to transmit a signal by acting on another cell (Paul and Snyder, 2012; Kabil et al., 2014). Although consensus has not been reached on the plasma sulfide concentrations (Olson, 2009), the released sulfide may carry information about the pH balance of sulfide-generating cells in the form of fractionated sulfur isotopic composition, because only the fully-protonated H_2S(aq) can diffuse freely across the membrane and pH determines the sulfur isotope partitioning between H_2S(aq) and HS^-(aq).

5. CONCLUSIONS

The equilibrium partitioning of sulfur isotopes between H_2S(aq) and HS^- affects the isotopic fractionations of a host of biotic and abiotic reactions involving sulfide. This arises because many reactions preferentially use either H_2S(aq) or HS^-(aq) as reactant, and the two differ in isotopic composition at equilibrium. Prior experimental investigations had yielded different estimates for this equilibrium fractionation ($\varepsilon_{HS\text{-}H2S}$), ranging from −2 to −6‰, apparently because of inadequate consideration of the effects of ionic strength on speciation of dissolved sulfide. In this study, we measured equilibrium fractionations at low ionic strength, using a new analytical approach (MC-ICP-MS), and thus avoid related artifacts. We estimate the enrichment factors for volatilization ($\varepsilon_{g\text{-}H2S}$) and deprotonation ($\varepsilon_{HS\text{-}H2S}$) of H_2S as −0.7‰ and −3.1‰, respectively. The new values are supported by the linearity of experimental data in $\alpha_{g\text{-}H2S}/\alpha_{g\text{-}aq}$ vs. $(1-X)$ plots, and are consistent with the recent theoretical estimates of −1‰ and −3.3‰ calculated by the B3LYP density functional method (Eldridge et al., 2016). The excellent agreement between

experiment and theory also suggests that the temperature dependence of DFT calculations is accurate. When combined, these studies provide a complete description of the temperature-dependent fractionation between H_2S(g), H_2S(aq), and HS^-(aq).

ACKNOWLEDGEMENTS

This research was supported by Basic Science Research Program through the National Research Foundation of Korea (NRF) funded by the Ministry of Education (No.2018R1-D1A1B07050970) and an Agouron Geobiology Fellowship to MSS, Gordon and Betty Moore Foundation Grant GBMF 3306 to VJO and ALS, NSF award OCE-1436566 to ALS and NSF award OCE-1340174 to JFA. The authors are grateful to Guillaume Paris for assistance for isotope analysis. We also thank Daniel Eldridge, Boswell Wing, and an anonymous reviewer for constructive comments on an earlier version of this manuscript.

REFERENCES

Amrani A., Kamyshny A., Lev O. and Aizenshtat Z. (2006) Sulfur stable isotope distribution of polysulfide anions in an $(NH_4)_2S_n$ aqueous solution. *Inorg. Chem.* **45**, 1427–1429.

Bates T. S., Lamb B. K., Guenther A., Dignon J. and Stoiber R. E. (1992) Sulfur emissions to the atmosphere from natural sources. *J. Atmos. Chem.* **14**, 315–337.

Baune C. and Böttcher M. E. (2010) Experimental investigation of sulphur isotope partitioning during outgassing of hydrogen sulphide from diluted aqueous solutions and seawater. *Isotopes Environ. Health Stud.* **46**, 444–453.

Berner R. A. (1984) Sedimentary pyrite formation: an update. *Geochim. Cosmochim. Acta* **48**, 605–615.

Berner R. A. (1989) Biogeochemical cycles of carbon and sulfur and their effect on atmospheric oxygen over Phanerozoic time. *Glob. Planet. Change* **1**, 97–122.

Brabec M. Y., Lyons T. W. and Mandernack K. W. (2012) Oxygen and sulfur isotope fractionation during sulfide oxidation by anoxygenic phototrophic bacteria. *Geochim. Cosmochim. Acta* **83**, 234–251.

Brunner B. et al. (2013) Nitrogen isotope effects induced by anammox bacteria. *Proc. Natl. Acad. Sci.* **110**, 18994–18999.

Buchwald C. and Casciotti K. L. (2010) Oxygen isotopic fractionation and exchange during bacterial nitrite oxidation. *Limnol. Oceanogr.* **55**, 1064–1074.

Canfield D. E. and Raiswell R. (1999) The evolution of the sulfur cycle. *Am. J. Sci.* **299**, 697–723.

Casciotti K. L. (2009) Inverse kinetic isotope fractionation during bacterial nitrite oxidation. *Geochim. Cosmochim. Acta* **73**, 2061–2076.

Chambers L. A. and Trudinger P. A. (1979) Microbiological fractionation of stable sulfur isotopes: a review and critique. *Geomicrobiol. J.* **1**, 249–293.

Cline J. D. (1969) Spectrophotometric determination of hydrogen sulfide in natural waters. *Limnol. Oceanogr.* **14**, 454–458.

Clayton R. N. and Kieffer S. W. (1991) Oxygen isotopic thermometer calibrations. In *Stable Isotope Geochemistry: A Tribute to Samuel Eustein*, vol. 3 (eds. H. P. Taylor, J. R. O'Neil and I. R. Kaplan). Geochem. Soc. Spec. Publ., San Antonio, pp. 3–10.

Czarnacki M. and Hałas S. (2012) Ab initio calculations of sulfur isotope fractionation factor for H_2S in aqua–gas system. *Chem. Geol.* **318**, 1–5.

Czyzewski B. K. and Wang D. N. (2012) Identification and characterization of a bacterial hydrosulphide ion channel. *Nature* **483**, 494.

Ding T., Valkiers S., Kipphardt H., De Bievre P., Taylor P. D. P., Gonfiantini R. and Krouse R. (2001) Calibrated sulfur isotope abundance ratios of three IAEA sulfur isotope reference materials and V-CDT with a reassessment of the atomic weight of sulfur. *Geochim. Cosmochim. Acta* **65**, 2433–2437.

Eigen M. and Kustin K. (1960) The influence of steric factors in fast protolytic reactions as studied with HF, H_2S and substituted phenols. *J. Am. Chem. Soc.* **82**, 5952–5953.

Eldridge D. L., Guo W. and Farquhar J. (2016) Theoretical estimates of equilibrium sulfur isotope effects in aqueous sulfur systems: highlighting the role of isomers in the sulfite and sulfoxylate system. *Geochim. Cosmochim. Acta* **195**, 171–200.

Ellis A. J. and Giggenbach W. (1971) Hydrogen sulphide ionization and sulphur hydrolysis in high temperature solution. *Geochim. Cosmochim. Acta* **35**, 247–260.

Fry B., Gest H. and Hayes J. M. (1984) Isotope effects associated with the anaerobic oxidation of sulfide by the purple photosynthetic bacterium. *Chromatium vinosum. FEMS Microbiol. Lett.* **22**, 283–287.

Fry B., Gest H. and Hayes J. M. (1986a) Sulfur isotope effects associated with protonation of HS^- and volatilization of H_2S. *Chem. Geol.* **58**, 253–258.

Fry B., Cox J., Gest H. and Hayes J. M. (1986b) Discrimination between ^{34}S and ^{32}S during bacterial metabolism of inorganic sulfur compounds. *J. Bacteriol.* **165**, 328–330.

Geßler R. and Gehlen K. V. (1986) Investigation of sulfur isotope fractionation between H_2S gas and aqueous solutions. *Fresenius' Zeitschrift für analytische Chemie* **324**, 130–136.

Giggenbach W. (1971) Optical spectra of highly alkaline sulfide solutions and the second dissociation constant of hydrogen sulfide. *Inorg. Chem.* **10**, 1333–1338.

Goffredi S. K., Childress J. J., Desaulniers N. T. and Lallier F. J. (1997) Sulfide acquisition by the vent worm *Riftia pachyptila* appears to be via uptake of HS, rather than H_2S. *J. Exp. Biol.* **200**, 2609–2616.

Hayes J. M. (2004) *An introduction to isotopic calculations*. Woods Hole Oceanographic Institution, Woods Hole.

Hershey J. P., Plese T. and Millero F. J. (1988) The pK_1* for the dissociation of H_2S in various ionic media. *Geochim. Cosmochim. Acta* **52**, 2047–2051.

Housecroft C. E. and Constable E. C. (2002) *Chemistry*, second ed. Prentice Hall, Harlow.

Jans U. and Miah M. H. (2003) Reaction of chlorpyrifos-methyl in aqueous hydrogen sulfide/bisulfide solutions. *J. Agric. Food Chem.* **51**, 1956–1960.

Jørgensen B. B. and Nelson D. C. (2004) Sulfide oxidation in marine sediments: geochemistry meets microbiology. In *Sulfur Geochemistry: Past and Present* (eds. J. P. Amend, K. J. Edwards and T. W. Lyons). Geological Society of America, Boulder, pp. 63–81.

Kabil O., Motl N. and Banerjee R. (2014) H_2S and its role in redox signaling. *Biochim Biophys. Acta, Proteins Proteom.* **1844**, 1355–1366.

Li L., Rose P. and Moore P. K. (2011) Hydrogen sulfide and cell signaling. *Annu. Rev. Pharmacol. Toxicol.* **51**, 169–187.

Licht S., Longo K., Peramunage D. and Forouzan F. (1991) Conductometric analysis of the second acid dissociation constant of H_2S in highly concentrated aqueous media. *J. Electroanal. Chem. Interfacial Electrochem.* **318**, 111–129.

Lide D. R. (2006) *CRC Handbook of Chemistry and Physics: A Ready-reference Book of Chemical and Physical Data*, 87th ed. CRC Press, Boca Raton.

Mathai J. C., Missner A., Kügler P., Saparov S. M., Zeidel M. L., Lee J. K. and Pohl P. (2009) No facilitator required for membrane transport of hydrogen sulfide. *Proc. Nat. Acad. Sci.* **106**, 16633–16638.

Migdisov A. A., Williams-Jones A. E., Lakshtanov L. Z. and Alekhin Y. V. (2002) Estimates of the second dissociation constant of H2S from the surface sulfidation of crystalline sulfur. *Geochim. Cosmochim. Acta* **66**, 1713–1725.

Morse J. W., Millero F. J., Cornwell J. C. and Rickard D. (1987) The chemistry of the hydrogen sulfide and iron sulfide systems in natural waters. *Earth Sci. Rev.* **24**, 1–42.

Olson K. R. (2009) Is hydrogen sulfide a circulating "gasotransmitter" in vertebrate blood? *Biochim. Biophys. Acta Bioenerg.* **1787**, 856–863.

Otake T., Lasaga A. C. and Ohmoto H. (2008) Ab initio calculations for equilibrium fractionations in multiple sulfur isotope systems. *Chem. Geol.* **249**, 357–376.

Paris G., Sessions A. L., Subhas A. V. and Adkins J. F. (2013) MC-ICP-MS measurement of $\delta^{34}S$ and $\Delta^{33}S$ in small amounts of dissolved sulfate. *Chem. Geol.* **345**, 50–61.

Paris G., Adkins J. F., Sessions A. L., Webb S. M. and Fischer W. W. (2014) Neoarchean carbonate–associated sulfate records positive $\Delta^{33}S$ anomalies. *Science* **346**, 739–741.

Paul B. D. and Snyder S. H. (2012) H_2S signalling through protein sulfhydration and beyond. *Nat. Rev. Mol. Cell Biol.* **13**, 499–507.

Raven M. R., Sessions A. L., Fischer W. W. and Adkins J. F. (2016) Sedimentary pyrite $\delta^{34}S$ differs from porewater sulfide in Santa Barbara Basin: Proposed role of organic sulfur. *Geochim. Cosmochim. Acta* **186**, 120–134.

Rickard D. and Luther, III, G. W. (1997) Kinetics of pyrite formation by the H_2S oxidation of iron (II) monosulfide in aqueous solutions between 25 and 125 °C: the mechanism. *Geochim. Cosmochim. Acta* **61**, 135–147.

Rickard D. and Luther, III, G. W. (2006) Metal sulfide complexes and clusters. *Rev. Mineral. Geochem.* **61**, 421–504.

Sim M. S., Bosak T. and Ono S. (2011) Large sulfur isotope fractionation does not require disproportionation. *Science* **333**, 74–77.

Sim M. S., Paris G., Adkins J. F., Orphan V. J. and Sessions A. L. (2017) Quantification and isotopic analysis of intracellular sulfur metabolites in the dissimilatory sulfate reduction pathway. *Geochim. Cosmochim. Acta* **206**, 57–72.

Schoonen M. A. A. and Barnes H. L. (1988) An approximation of the second dissociation constant for hydrogen sulfide. *Geochim. Cosmochim. Acta* **52**, 649–654.

Schauble E. A. (2004) Applying stable isotope fractionation theory to new systems. *Rev. Mineral. Geochem.* **55**, 65–111.

Szabo C., Coletta C., Chao C., Módis K., Szczesny B., Papapetropoulos A. and Hellmich M. R. (2013) Tumor-derived hydrogen sulfide, produced by cystathionine-β-synthase, stimulates bioenergetics, cell proliferation, and angiogenesis in colon cancer. *Proc. Nat. Acad. Sci.* **110**, 12474–12479.

Thamdrup B., Fossing H. and Jørgensen B. B. (1994) Manganese, iron and sulfur cycling in a coastal marine sediment, Aarhus Bay, Denmark. *Geochim. Cosmochim. Acta* **58**, 5115–5129.

Tostevin R., Turchyn A. V., Farquhar J., Johnston D. T., Eldridge D. L., Bishop J. K. and McIlvin M. (2014) Multiple sulfur isotope constraints on the modern sulfur cycle. *Earth Planet. Sci. Lett.* **396**, 14–21.

Yongsiri C., Vollertsen J. and Hvitved-Jacobsen T. (2005) Influence of wastewater constituents on hydrogen sulfide emission in sewer networks. *J. Environ. Eng.* **131**(2), 1676–1683.

Zhang J., Wang L. and Yang Z. (2004) Emission of biogenic sulfur gases from the microbial decomposition of cystine in Chinese rice paddy soils. *Bull. Environ. Contam. Toxicol.* **72**, 850–857.

Zerkle A. L., Farquhar J., Johnston D. T., Cox R. P. and Canfield D. E. (2009) Fractionation of multiple sulfur isotopes during phototrophic oxidation of sulfide and elemental sulfur by a green sulfur bacterium. *Geochim. Cosmochim. Acta* **73**, 291–306.

Associate editor: Jeffrey C. Alt